10244 *Inorg. Chem.* **2010**, *49*, 10244–10246
DOI: 10.1021/ic1018949

Inorganic Chemistry
Communication

Fabrication of Apatite-Type $La_{9.33}(SiO_4)_6O_2$ Hollow Nanoshells as Energy-Saving Oxidative Catalysts

Xian-Hua Zhang,*,†,‡ Xiaodong Yi,† Jiawei Zhang,† Zhaoxiong Xie,*,† Junyong Kang,‡ and Lansun Zheng†

†*State Key Laboratory for Physical Chemistry of Solid Surfaces, Department of Chemistry, College of Chemistry and Chemical Engineering,* ‡*Fujian Key Laboratory of Semiconductor Materials and Applications, Department of Physics, Xiamen University, Xiamen 361005 China*

Received September 15, 2010

Apatite-type $La_{9.33}(SiO_4)_6O_2$ hollow nanoshells were successfully synthesized by a controlled route. These oxide-ion-conducting hollow nanoshells were used to catalyze oxidative coupling of methane, and an enhanced catalytic performance at relatively low temperature was realized. The high-activity and energy-saving features were attributed to their hollow nanostructures and oxide ion conductivity.

Recently, apatite-type lanthanide (Ln)-silicates have been reported to be a new family of oxide ion conductors at moderate temperatures.[1,2] These materials have the general formula of $Ln_{10-x}(SiO_4)_6O_{2+y}$ (Ln = La, Nd, Gd, Dy, etc.).[3] The oxide ion conductivity of apatite-type Ln-silicates is attributed to the crystal structure, which comprises isolated SiO_4 tetrahedra arranged so as to form two distinct channels running parallel to the *c* axis. Occupying the smaller of these channels are Ln cations, while the larger channel contains oxide ions. Moreover, it is found that apatite-type Ln-silicates are tolerant of an unusually broad range of dopants, particularly on the Ln sites, with the oxide ion conductivity being very sensitive to the doping regime and cation/anion nonstoichiometry.[4−8] Therefore, these oxide ion conductors are promising functional materials with tunable properties. To date, a number of apatite-type Ln-silicates have been reported, such as $La_{10}Si_6O_{27}$, $La_{9.33}(SiO_4)_6O_2$, and their doped compounds. Especially, $La_{9.33}(SiO_4)_6O_2$ with La vacancies in the small channels has attracted growing interest because of its high oxide ion conductivity.[9−11] In practical applications, the apatite-type Ln-silicates are proposed as alternative solid electrolyte materials, which exhibit excellent oxide ion conductivity at relatively low temperatures and low oxygen partial pressures.[12−15] However, as a new type of oxide ion conductor, their properties and potential applications based on nanostructures remain to be investigated.

Well-crystalline apatite-type silicates are usually formed under high-temperature conditions (> 800 °C). The high-temperature condition is a challenge in the fabrication of nanostructures of apatite-type silicates, which vulnerably leads to the collapse of nanostructures.[16] To the best of our knowledge, well-crystalline apatite-type Ln-silicate nanostructures have rarely been reported. Herein, apatite-type $La_{9.33}(SiO_4)_6O_2$ hollow nanoshells are successfully synthesized by a controlled route. These oxide-ion-conducting hollow nanoshells are used as energy-saving catalysts for the oxidative coupling of menthane (OCM). An enhanced catalytic performance at relatively low temperature is realized, and the high activity for the OCM reaction is attributed to their high oxide ion conductivity and hollow nanostructures. Moreover, the silicate hollow nanoshells are stable at high temperature (> 800 °C) and are potential high-efficiency catalysts for other high-temperature oxidative reactions.

In typical procedures (Scheme S1 in the Supporting Information, SI), spherical La-hydroxide precursors are first synthesized. Second, the precursor spheres are wrapped by silica to form core−shell structures.[17,18] Third, at an elevated

*To whom correspondence should be addressed. E-mail: xhzhang@xmu.edu.cn (X.H.Zhang), zxxie@xmu.edu.cn (Z.X.Xie). Tel: +86-592-2180627. Fax: +86-592-2183047.

(1) Nakayama, S.; Kageyama, T.; Aono, H.; Sadaoka, Y. *J. Mater. Chem.* **1995**, *5*, 1801.
(2) Nakayama, S.; Sakamoto, M. *J. Eur. Ceram. Soc.* **1998**, *18*, 1413.
(3) Martínez-González, L. G.; Rodríguez-Reyna, E.; Moreno, K. J.; Escalante-García, J. I.; Fuentes, A. F. *J. Alloys Compd.* **2009**, *476*, 710.
(4) Abram, E. J.; Sinclair, D. C.; West, A. R. *J. Mater.Chem.* **2001**, *11*, 1978.
(5) Tolchard, J. R.; Islam, M. S.; Slater, P. R. *J. Mater. Chem.* **2003**, *13*, 1956.
(6) Najib, A.; Sansom, J. E. H.; Tolchard, J. R.; Slater, P. R.; Islam, M. S. *Dalton Trans.* **2004**, 3106.
(7) Tolchard, J. R.; Slater, P. R.; Islam, M. S. *Adv. Funct. Mater.* **2007**, *17*, 2564.
(8) Jacobson, A. J. *Chem. Mater.* **2010**, *22*, 660.
(9) Nakayama, S.; Aono, H.; Sakaokac, Y. *Chem. Lett.* **1995**, *6*, 43.
(10) Okudera, H.; Masubuchi, Y.; Kikkawa, S.; Yoshiasa, A. *Solid State Ionics* **2005**, *176*, 1473.
(11) Iwata, T.; Fukuda, K.; Béchade, E.; Masson, O.; Julien, I.; Champion, E.; Thomas, P. *Solid State Ionics* **2007**, *178*, 1523.
(12) Ormerod, R. M. *Chem. Soc. Rev.* **2003**, *32*, 17.
(13) Mamak, M.; Metraux, G. S.; Petrov, S.; Coombs, N.; Ozin, G. A.; Green, M. A. *J. Am. Chem. Soc.* **2003**, *125*, 5161.
(14) Shao, Z. P.; Haile, S. M. *Nature* **2004**, *431*, 170.
(15) Tao, S.; Irvine, J. T. S.; Kilner, J. A. *Adv. Mater.* **2005**, *17*, 1734.
(16) Huang, C. C.; Huang, W.; Su, C. H.; Feng, C. N.; Kuo, W. S.; Yeh, C. S. *Chem. Commun.* **2009**, 3360.
(17) Liz-Marzán, L. M.; Giersig, M.; Mulvaney, P. *Langmuir* **1996**, *12*, 4329.
(18) Zhao, X. J.; Bagwe, R. P.; Tan, W. H. *Adv. Mater.* **2004**, *16*, 173.

Published on Web 10/11/2010

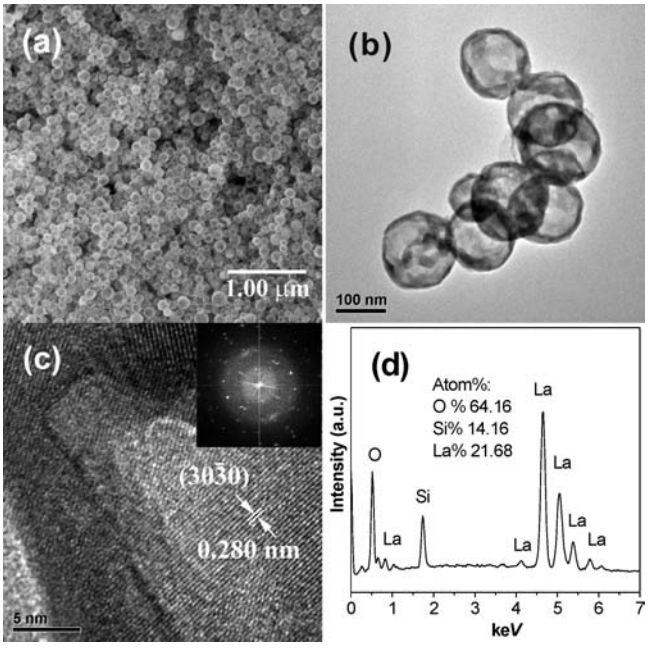

Figure 1. SEM (a) and TEM (b) images of the Ln-silicate hollow nanoshells. (c) HRTEM image with FFT analysis (inset) of the silicate nanoshells. (d) EPMA results of the $La_{9.33}(SiO_4)_6O_2$ hollow nanoshells.

temperature, the precursors decompose and diffuse to form hollow nanostructures, while the resulting La-oxides react with silica shells to form apatite-type silicate hollow nanoshells at high temperature (850 °C). Finally, the amorphous silica outer shells are removed by adding an excess of a sodium hydroxide solution. It should be pointed out that the silica shells are used as both reactants and hard templates for outer-space limitation. Therefore, high-temperature calcination is allowed in our strategy. The obtained silicate hollow nanoshells are well-crystalline, which is better than the previous low-crystallinity silicate nanoshells.[19,20] Moreover, this synthetic strategy can be extended to fabricate the other well-crystalline silicate nanostructures (Figure S8 in the Supporting Information).

Figure 1a shows the scanning electron microscopy (SEM) image of the La-silicate hollow nanoshells. The mean diameter of the nanoshells is determined to be ~150 nm by measuring more than 100 nanoshells. The transmission electron microscopy (TEM) image of nanoshells further determines the hollow nanostructure, and the shell thickness is about 10 nm (Figure 1b). The high-resolution TEM (HRTEM) image (Figure 1c) and the corresponding fast Fourier transform (FFT) analysis (inset of Figure 1c) reveal well-crystalline structures in the shell component. As shown in Figure 2, the powder X-ray diffraction (XRD) pattern of the as-prepared hollow nanoshells clearly exhibits diffraction peaks, which match well with hexagonal $La_{9.33}(SiO_4)_6O_2$ (JCPDS no. 49-0443). Moreover, the XRD pattern is also consistent with the simulated results for apatite-type $La_{9.33}(SiO_4)_6O_2$ reported by León-Reina et al.[21] To exclude the possibility of $La_{10}Si_6O_{27}$, electron probe microanalysis (EPMA) is carried

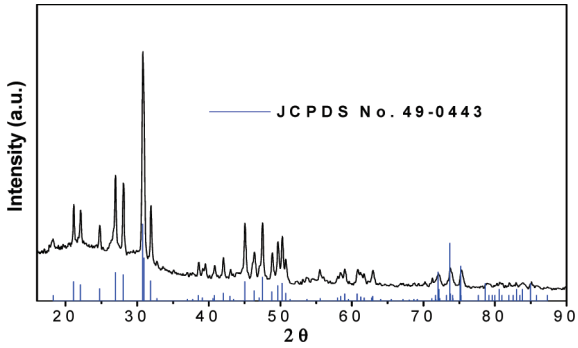

Figure 2. XRD pattern of the as-prepared Ln-silicate hollow nanoshells, in which the blue lines represent the standard data for hexagonal $La_{9.33}(SiO_4)_6O_2$ (JCPDS no. 49-0443).

out. As shown in Figure 1d, the atomic ratio of Si/La is determined to be about 0.65 which is in good agreement with the calculated value (0.64) for $La_{9.33}(SiO_4)_6O_2$. Consequently, we could draw a conclusion that the hollow nanoshells are well-crystalline apatite-type $La_{9.33}(SiO_4)_6O_2$. In addition, the N_2 isotherms of the hollow apatite nanoshells are recorded, which can be categorized as type IV with a distinct hysteresis loop (Figure S3 in the SI). The Brunauer−Emmett−Teller surface area of the nanoshells is calculated to be about 42.5 $m^2\ g^{-1}$. The high surface area for the silicate nanoshells is attributed to their hollow nanostructures.

Hollow nanostructures with high specific surface area, low density, and well permeation can be used as nanoreactors for catalytic applications.[22] The oxide-ion-conducting $La_{9.33}(SiO_4)_6O_2$ hollow nanoshells are regarded as promising high-activity oxidative catalysts. We hope that the fast exchange of oxygen ions in the apatite-type $La_{9.33}(SiO_4)_6O_2$ may benefit the oxidative process. Herein, high-temperature OCM reaction is selected as the model reaction to examine the catalytic performance of the nanoshells. The OCM reaction has been used in the last decades to produce C_{2+} hydrocarbons, mainly C_2H_6 and C_2H_4.[23−28] To date, the highest C_2 yield reported is up to ~26%.[27] To achieve commercialization of OCM, effort in developing high-activity catalysts is still needed. However, most of the previous works to improve the C_2 yield and selectivity were carried out under high-temperature conditions (> 600 °C). In fact, high energy consumption is also a challenge to the commercialization of OCM. At present, energy-saving materials and technologies are becoming more and more important because of the increasing requirement for environmental protection. Therefore, we mainly focused on developing high-activity catalysts for OCM at relatively low temperature. The catalytic activities of $La_{9.33}(SiO_4)_6O_2$ hollow nanoshells toward the OCM reaction are tested within the temperature range of 400−600 °C.

The catalytic activities of $La_{9.33}(SiO_4)_6O_2$ hollow nanoshells for OCM are summarized in Table 1. As expected, the high catalytic activities for the OCM reaction are testified to at low temperature. The startup temperature for OCM is as

(19) Guo, Z. Y.; Du, F. L.; Li, G. C.; Cui, Z. L. *Chem. Commun.* **2008**, 2911.
(20) Wang, Y. Q.; Wang, G. Z.; Wang, H. Q.; Cai, W. P.; Zhang, L. D. *Chem. Commun.* **2008**, 6555.
(21) León-Reina, L.; Losilla, E. R.; Martinez-Lara, M.; Bruque, S.; Llobert, A.; Sheptyakov, D. V.; Aranda, M. A. G. *J. Mater. Chem.* **2005**, *15*, 2489.
(22) Liang, X.; Xiao, J. J.; Chen, B. H.; Li, Y. D. *Inrog. Chem.* **2010**, *49*, 8188.
(23) Keller, G. E.; Bhasin, M. M. *J. Catal.* **1982**, *73*, 9.
(24) Ito, T.; Lunsford, J. H. *Nature* **1985**, *314*, 721.
(25) Driscoll, D. J.; Martir, W.; Wang, J. X.; Lunsford, J. H. *J. Am. Chem. Soc.* **1985**, *107*, 58.
(26) Long, R. Q.; Wan, H. L. *Appl. Catal., A* **1997**, *159*, 45.
(27) Takanabe, K.; Iglesia, E. *J. Phys. Chem. C* **2009**, *113*, 10131.
(28) Taheri, Z.; Seyed-Matin, N.; Safekordi, A. A.; Nazari, K.; Pashne, S. Z. *Appl. Catal., A* **2009**, *354*, 143.

Table 1. Catalytic Activities for the OCM Reaction Catalyzed by $La_{9.33}(SiO_4)_6O_2$ Nanocatalysts[a]

		selectivity (%)					
T (°C)	CH_4 convn (%)	CO	CO_2	C_2H_4	C_2H_6	C_2	C_2 yield (%)
400	5.4	11.2	52.6	18.3	17.9	36.2	2.0
450	27.8	19.4	37.9	20.9	21.8	42.7	11.9
500	29.6	18.0	36.6	22.4	23.0	45.4	13.4
550	31.4	15.7	37.8	23.2	23.3	46.5	14.6
600	33.4	7.5	42.1	25.6	24.8	50.4	16.8

[a] Reaction conditions: CH_4/O_2 molar ratio = 3:1; GHSV = 7500 mL g^{-1} h^{-1}; catalyst weight = 400 mg. The data were recorded after 30 min on stream.

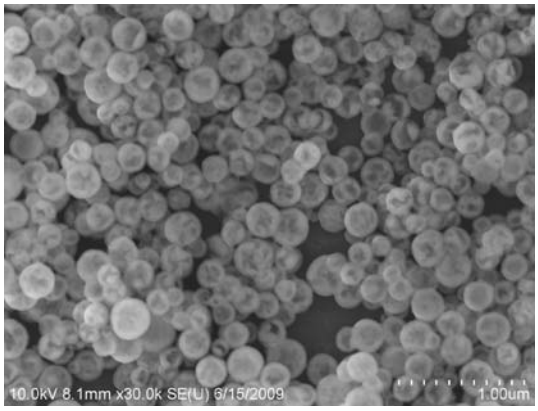

Figure 3. SEM image of the $La_{9.33}(SiO_4)_6O_2$ hollow nanoshells over one catalytic cycle.

low as 400 °C. Compared with the previous high-activity catalysts, for example, Fallah and Falamaki reported a new nano-$2Li_2O$/MgO catalyst/porous α-alumina composite for the OCM reaction. They reported that the C_2 yield at 750 °C was as high as 25% (C_2 selectivity ∼ 60%);[29] however, no catalytic activity at 400 °C was reported, and the C_2 yield at 500 °C was just ∼7%. As to the hollow nanoshells in our catalytic experiments, the C_2 yield reaches 13.4% at 500 °C. Obviously, $La_{9.33}(SiO_4)_6O_2$ hollow nanoshells exhibit high activities for OCM at relatively low temperature. In addition, as shown in Figure 3, the $La_{9.33}(SiO_4)_6O_2$ hollow nanoshells over one catalytic cycle preserve their hollow nanostructures perfectly, testifying to their high-temperature stability. Moreover, almost no carbon deposits are seen, showing their high catalytic efficiency and recycling behavior. Further high-temperature tests indicate that the hollow nanoshells can keep their hollow nanostructures at temperatures as high as 800 °C (Figure S5 in the SI). These high-activity and high-temperature stable nanocatalysts are potential candidates for other high-temperature oxidative processes (Figure S7 in the SI).

(29) Fallah, B.; Falamak, C. *AIChE J.* **2010**, *56*, 717.

On the basis of the previous reports on the catalytic mechanism for OCM,[30−35] the heterogeneous−homogeneous process for the OCM reaction has been generally accepted as the following steps: (i) a methane molecule reacts with a surface oxygen species to produce a gaseous methyl radical ($CH_3^{\bullet}$) as the rate-limiting step; (ii) the methyl radical subsequently couples with another methyl radical in the gas phase to form ethane; (iii) further dehydrogenation of ethane to form ethene takes place in the gas phase or on the surface of the catalysts. The surface oxygen species (e.g., O_2^-, O_2^{2-}, O^-) are supposed to be essential for C−H bond cleavage to produce methyl radicals. As to the $La_{9.33}(SiO_4)_6O_2$ nanocatalysts, a high C_2 yield at relatively low temperature (16.8% at 600 °C) is obtained. This high-efficiency catalytic performance for OCM is related to its high-surface-area hollow nanostructure, which can absorb reactants and active oxygen species acting as nanoreactors. Moreover, the high oxide ion conductivity of the apatite-type silicates, which benefits oxygen permeation and diffusion, might play an important role in the oxidative process. To determine the detailed mechanism, further investigation based on theoretical simulations and catalytic experiments is still needed.

In summary, apatite-type $La_{9.33}(SiO_4)_6O_2$ hollow nanoshells were successfully synthesized by a controlled route. Well-crystalline $La_{9.33}(SiO_4)_6O_2$ hollow nanoshells with high oxide ion conductivity and special surface area were applied in the OCM reaction as energy-saving nanocatalysts. An enhanced catalytic performance for OCM catalyzed by the hollow nanoshells at relatively low temperature was testified to, which is attributed to their hollow nanostructures and oxide ion conductivity.

Acknowledgment. This work was supported by the National Natural Science Foundation of China (Grants 20725310 and 20721001), Key Scientific Project of Fujian Province of China (Grant 2009HZ0002-1), the National Basic Research Program of China (Grants 2007CB815303 and 2009CB939804), and China Postdoctoral Science Foundation (Grant D05011).

Supporting Information Available: Experimental details, N_2 isotherms, SEM and STEM images, catalytic activities, high-temperature tests, and an XRD pattern. This material is available free of charge via the Internet at http://pubs.acs.org.

(30) Ito, T.; Wang, J. X.; Lin, C. H.; Lunsford, J. H. *J. Am. Chem. Soc.* **1985**, *107*, 5062.
(31) Campbell, K. D.; Lunsford, J. H. *J. Phys. Chem.* **1988**, *92*, 5792.
(32) Morales, E.; Lunsford, J. H. *J. Catal.* **1989**, *118*, 255.
(33) Nelson, P. F.; Lukey, C. A.; Cant, N. W. *J. Phys. Chem.* **1988**, *92*, 6176.
(34) Labinger, J. A.; Ott, K. C. *J. Phys. Chem.* **1987**, *91*, 2682.
(35) Wang, L. H.; Yi, X. D.; Weng, W. Z.; Wan, H. L. *Catal. Today* **2008**, *131*, 135.